



BNL-216090-2020-JAAM

The ARM Data-oriented Metrics and Diagnostics Package for Climate Models

C. Zhang, W. Lin

To be published in "Bulletin of the American Meteorological Society"

June 2020

Environmental and Climate Sciences Department
Brookhaven National Laboratory

U.S. Department of Energy

USDOE Office of Science (SC), Biological and Environmental Research (BER) (SC-23)

Notice: This manuscript has been authored by employees of Brookhaven Science Associates, LLC under Contract No. DE-SC0012704 with the U.S. Department of Energy. The publisher by accepting the manuscript for publication acknowledges that the United States Government retains a non-exclusive, paid-up, irrevocable, world-wide license to publish or reproduce the published form of this manuscript, or allow others to do so, for United States Government purposes.

DISCLAIMER

This report was prepared as an account of work sponsored by an agency of the United States Government. Neither the United States Government nor any agency thereof, nor any of their employees, nor any of their contractors, subcontractors, or their employees, makes any warranty, express or implied, or assumes any legal liability or responsibility for the accuracy, completeness, or any third party's use or the results of such use of any information, apparatus, product, or process disclosed, or represents that its use would not infringe privately owned rights. Reference herein to any specific commercial product, process, or service by trade name, trademark, manufacturer, or otherwise, does not necessarily constitute or imply its endorsement, recommendation, or favoring by the United States Government or any agency thereof or its contractors or subcontractors. The views and opinions of authors expressed herein do not necessarily state or reflect those of the United States Government or any agency thereof.

27 **ABSTRACT.** The U.S. Department of Energy (DOE) Atmospheric Radiation Measurement
28 (ARM) program produces ground-based long-term contiguous unique measurements for
29 atmospheric state, precipitation, turbulent fluxes, radiation, aerosol, cloud and the land surface,
30 which are collected at its multiple Climate Research Facilities. These comprehensive datasets have
31 been widely used to calibrate climate models and are proven to be invaluable for climate model
32 development and improvement. This article introduces an evaluation package to facilitate the use
33 of ground-based ARM measurements in climate model evaluation.

34
35 The ARM data-oriented metrics and diagnostics package (ARM-DIAGS) includes both ARM
36 observational datasets and a Python-based analysis toolkit for computation and visualization. The
37 observational datasets are compiled from multiple ARM data products and specifically tailored for
38 use in climate model evaluation. In addition, ARM-DIAGS also includes simulation data from
39 models participating the Coupled Model Inter-comparison Project (CMIP), which will allow
40 climate-modeling groups to compare a new, candidate version of their model to existing CMIP
41 models. The analysis toolkit is designed to make the metrics and diagnostics quickly available to
42 the model developers.

43

44 **1. Introduction**

45 A set of standard metrics and diagnostics provides an effective way for climate modeling
46 centers to routinely assess their model performance and judge the improvement of model
47 simulations from new parameterizations. In the past, climate model developers have often relied
48 on satellite remote sensing products to calibrate and tune their models. Satellite data sets provide
49 a great global coverage, however, it is difficult to apply satellite data in some process studies due
50 to their poor temporal resolutions. Therefore, utilizing detailed high-frequency ground-based
51 measurements for a comprehensive collection of quantities can be a complementary test in model
52 evaluation.

53 Over the past three decades, the U.S. Department of Energy (DOE) Atmospheric Radiation
54 Measurement (ARM) program has established several permanent research sites and deployed a
55 number of ARM Mobile Facilities (AMF) in diverse climate regimes around the world to collect
56 long-term continuous field measurements of clouds, aerosols, and radiation and their associated
57 large-scale environments. These detailed field observations have provided a unique observational
58 basis specifically for understanding cloud and precipitation related processes and evaluating and
59 improving their representations in climate models. However, ARM data have not been extensively
60 utilized in current model development workflows. With the growing interest in the climate
61 modeling community in developing process-oriented metrics and diagnostics to aid
62 parameterization developments (Maloney et al. 2019), the high-frequency process-oriented ARM
63 observations should play a more important role in the future metrics and diagnostics development.

64 In this article, we introduce the recently developed ARM data-oriented metrics and diagnostics
65 package (ARM-DIAGS) for the global climate community to facilitate the use of ARM field data
66 in climate model evaluation. The focus is on ARM unique observations on clouds and aerosols, as

67 well as process-oriented diagnostics that are particularly aimed to improve the representation of
68 cloud and precipitation related processes in climate models, such as those included in the Coupled
69 Model Inter-comparison Project (CMIP). The package is available publicly with the hope that it
70 can serve as an easy entry point for climate modelers to compare their models with ARM data and
71 supplemented CMIP datasets.

72

73 **2. Overview of the ARM data-oriented metrics and diagnostics package**

74 The ARM-DIAGS development closely follows the CMIP protocol to efficiently distribute
75 ARM metrics and diagnostics package along with other metrics packages to the CMIP community
76 and other climate modeling centers. For this purpose, the diagnostic toolkit is built with the Python
77 programming language and utilizes Python libraries for scientific analysis (such as NumPy and
78 matplotlib). Additional Python packages developed by DOE (i.e., the Community Data Analysis
79 Tools (CDAT), <https://cdat.llnl.gov/>) are also used. Four components are currently included in the
80 ARM-DIAGS: 1) a Python-based analysis program; 2) an ARM-based collection of mean and
81 diurnal and seasonal cycle climatologies as well as high time frequency data for process-oriented
82 diagnostics; 3) a database of simulation data from models contributed to CMIP project; and 4)
83 relevant technical documentations for ARM-DIAGS.

84 The observations used to assess model performance primarily rely on the ARM Best Estimate
85 (ARMBE) data products (Xie et al. 2010) and other ARM value-added products (VAPs)
86 (<https://www.arm.gov/capabilities/vaps>), which are available for all the ARM permanent research
87 sites and some ARM mobile facilities. These data often rely on measurements at the ARM Central
88 Facility (CF) locations (i.e., single point measurements). To improve model-observation
89 comparison, the ARM long-term continuous forcing data (Xie et al. 2004), which represents an

90 average over a Global Climate Model (GCM) grid box, is also used when it is available. For cloud
91 properties such as cloud liquid and ice water contents, the ARM Cloud Retrieval Ensemble Data
92 (ACRED) (Zhao et al. 2012) is used. The detailed information about ARM data used in the ARM-
93 DIAGS package is listed in Tables 1a and 1b. The observational data product consists of hourly
94 averaged, diurnal cycle, monthly means or climatological summaries of the measured quantities,
95 with variable names, units and vertical dimensions remapped to CMIP convention. They are
96 currently available for the Southern Great Plains (SGP) site (Table 1a) as well as the North Slope
97 of Alaska (NSA) Barrow site and the Tropical Western Pacific (TWP) Manus, Nauru, and Darwin
98 sites (Table 1b). Other than the ARM observations, ARM-DIAGS also includes simulation data
99 from models participating CMIP project, which will allow climate-modeling groups to compare a
100 new candidate version of their model to existing CMIP models. A full list of metrics and
101 diagnostics are as follows, with a subset demonstrated in Section 3 of this article.

- 102 • A set of basic metrics tables: mean, mean bias, correlation and root mean square error
103 based on annual cycle of each variable.
- 104 • Line plots and Taylor Diagrams (Taylor, 2001) for annual cycle variability of each
105 variable.
- 106 • Contour and vertical profiles of annual cycle and diurnal cycle of cloud fraction.
- 107 • Line and harmonic dial plots (Covey et al. 2016) of diurnal cycle of precipitation.
- 108 • Probability Density Function plots of precipitation rate (Pendergrass et al. 2014)
- 109 • Convection onset metrics showing statistical relationship between precipitation rate
110 and column water vapor (Schiro et al. 2016)

111

112 **3. Facilitating use of ARM data in climate model evaluation**

113 *Diagnosis of summertime warm bias.* The data and diagnostics provided through ARM-DIAGS
114 have been used for studying the systematic warm bias in surface temperature found among the
115 climate models in summertime at mid-latitude continent including the ARM SGP site (Zhang et
116 al. 2018). The biases are consistent with both overestimated surface shortwave radiation and
117 underestimated evaporative fraction, which contribute to the warm bias as illustrated in Figure 1.
118 These diagnostics provide an integrated picture with detailed field observations to identify possible
119 model deficiency in representing cloud, radiation, and land properties, as well as their interactions.

120

121 *Diurnal cycle of cloud fraction:* This daily cycle could serve as a critical test of the models'
122 representation of the physical processes controlling cloud life cycle. One unique product from
123 ARM is cloud vertical profile measurements derived from an integration of multiple active remote
124 sensors, including Millimeter wavelength cloud radars, laser ceilometers and Micropulse Lidars
125 (Active Remote Sensing of Clouds product, ARSCL). Figure 2 shows a comparison between
126 observed and simulated diurnal cycle of cloud vertical structure over the ARM midlatitude and
127 tropical sites (i.e., SGP and Manus), where prominent climatological diurnal cycle of clouds is
128 present. Over the SGP site, a lack of shallow to deep cloud transition during summertime (June-
129 July-August) is shown in E3SM. This is a common model bias which is related to model deep
130 convection that is triggered too easily and does not allow low clouds to build-up. The Manus site
131 exhibits a strong diurnal cycle, with a maximum in low cloud fraction occurring at early local noon
132 and followed by a maximum in high cloud hours later. Similarly, the model in general
133 underestimated the lower cloud and overestimated high cloud, which is also lack of diurnal
134 variability.

135 *Diurnal cycle of precipitation.* Diurnal cycle of precipitation is often served as a benchmark for
136 climate models. The diurnal cycle diagnostics in ARM-DIAGS, which compare the precipitation
137 intensity and its peak time, have been utilized by the Energy Exascale Earth System Model (E3SM)
138 development team to assess the performance of a newly developed convection triggering
139 mechanism (Xie et al. 2019). Figure 3 shows that all climate models including the default E3SM
140 are not able to capture the observed nocturnal peak which is often associated with the eastward
141 propagation of mesoscale convective systems. A recently developed convective triggering
142 function, which incorporates an empirical dynamic constraint and allows elevated convection to
143 be captured, started to pick up the early morning peak time, although the intensity is still too weak.
144 These diagnostics are useful to repeat continually, especially when new features in convection
145 parameterizations are implemented.

146

147 *Precipitation distribution.* The probability density function analysis for daily mean precipitation
148 at the SGP site during June-July-August is shown in Figure 4. This example illustrates that models
149 tend to underestimate heavy rainfall (>10 mm per day) occurrences which contribute more to the
150 total precipitation amount than lighter rainfall occurrence. The overlaying result from GPCP
151 (Global Precipitation Climatology Project One-Degree Daily Precipitation Data Set) also confirms
152 this systematic model bias.

153

154 *Convection onset metrics.* Convection onset metrics allow users to compare diagnostics for the
155 behavior of deep convection from ARM observations to model output. The statistics quantify
156 robust relationships between precipitation, column water vapor (CWV) and temperature. This
157 includes the sharp increase or “pickup” in conditional-average precipitation rate above a critical
158 CWV value seen in Figure 5a, which is easily identifiable for short time averages at tropical ARM

159 sites. The pickup represents the onset of conditional instability yielding strong convective
160 precipitation (Schiro et al. 2016) and is also seen in the probability of precipitation (Figure 5b).
161 The probability density of CWV and the contribution from precipitating points (Figure 5c) have a
162 drop in probability density at high CWV corresponding to the regime with high precipitation loss
163 above critical.

164 The statistics discussed here can distinguish between models' convective parametrizations and
165 their qualitative characteristics are robust to space and time averaging (Kuo et al. 2018). An
166 example of model comparison is given in Figure 5. An important diagnostic in the model
167 evaluation of convection onset concerns the critical CWV value where the precipitation pickup
168 begins. Many models exhibit a pickup at lower CWV than observations (Kuo et al. 2020), as seen
169 in Figure 5a for E3SM. This mismatch persists even when temperature dependence (not shown but
170 will be included in a feature release of ARM-DIAGS) is included by binning by the saturation
171 water vapor.

172 173 **4. Summary and future work**

174 The ARM metrics and diagnostics package is designed and developed to facilitate the use of ARM
175 ground-based in-situ measurements in climate model evaluation. Metrics and diagnostics
176 evaluating the simulated atmospheric and cloud fields are generated by running a Python program
177 in a simple software environment based on CDAT. The v2.0 ARM-DIAGS's analysis codes are
178 currently publicly available through GitHub ([https://github.com/ARM-DOE/arm-gcm-](https://github.com/ARM-DOE/arm-gcm-diagnostics)
179 [diagnostics](https://github.com/ARM-DOE/arm-gcm-diagnostics)) under the ARM User Facility project space. Analysis data include ARM observational
180 datasets and the reference CMIP5 AMIP data can be downloaded through the ARM archive
181 (<https://www.arm.gov/capabilities/vaps/adcme-123>). For now, the default requirement for the

182 input model is that the data are under CMIP conventions. Anyone interested in applying ARM-
183 DIAGS to a specific model should contact the development team via our GitHub page for specific
184 configurations for a model run.

185 Future work includes extending the ARM-DIAGS to the ARM Eastern North Atlantic (ENA) site
186 (a new fixed site) and ARM AMF sites. CMIP6 data will be included as it becomes available. The
187 diagnostics suite will be continuously improved with close collaboration with scientists in the field.
188 Ongoing work includes incorporation of the recently developed ARM cloud radar simulator (Y.
189 Zhang et al. 2018) into ARM-DIAGS to improve the comparison between model clouds and ARM
190 cloud radar observations, as well as adding temperature dependence to convection onset statistics.
191 In addition, utilizing other sources of observations, such as those retrieved from satellites, as
192 supplementary data, can help address issues associated with observation uncertainty and data
193 resolution.

194

195 Acknowledgement: This research was supported by the DOE Atmospheric Radiation
196 Measurement (ARM) program and performed under the auspices of the U. S. Department of
197 Energy by Lawrence Livermore National Laboratory under contract No. DE-AC52-07NA27344.
198 IM release: LLNL-ABS-789643. Work at UCLA was supported by U.S. Department of Energy
199 Grant DE-SC0011074 and subcontract B634021 and National Science Foundation AGS-1540518,
200 AGS-1936810. We acknowledge the U.S. Department of Energy's Program for Climate Model
201 Diagnosis and Intercomparison to provide coordinating support and lead development of software
202 infrastructure in partnership with the Global Organization for Earth System Science Portals for
203 making CMIP data available.

204 **For Further Reading:**

205 Bond, D. (2005), Soil Water and Temperature System (SWATS) Handbook, ARM Technical
206 Report TR-063, U.S. Department of Energy, Washington, D. C.
207

208 Cook, D. R. (2011a). Energy Balance Bowen Ratio Station (EBBR) Handbook (No. DOE/SC-
209 ARM/TR-037). DOE Office of Science Atmospheric Radiation Measurement (ARM) Program
210 (United States).
211

212 Cook, D. R. (2011b). Eddy Correlation Flux Measurement System (ECOR) Handbook (No.
213 DOE/SC-ARM/TR-052). DOE Office of Science Atmospheric Radiation Measurement (ARM)
214 Program (United States).
215

216 Covey, C., Gleckler, P. J., Doutriaux, C., Williams, D. N., Dai, A., Fasullo, J., ... & Berg, A.
217 (2016). Metrics for the diurnal cycle of precipitation: Toward routine benchmarks for climate
218 models. *Journal of Climate*, 29(12), 4461-4471.
219

220 Clothiaux, E. E., T. P. Ackerman, G. G. Mace, K. P. Moran, R. T. Marchand, M. Miller, and B.
221 E. Martner, 2000: Objective determination of cloud heights and radar reflectivities using a
222 combination of active remote sensors at the ARM CART sites. *J. Appl. Meteor.*, 39, 645–665.
223

224 Chandra, A. S., C. Zhang, S. A. Klein, and H.-Y. Ma (2015), Low-cloud characteristics over the
225 tropical western Pacific from ARM observations and CAM5 simulations, *J. Geophys. Res. Atmos.*,
226 120, 8953–8970, doi:10.1002/2015JD023369.
227

228 Knootz, et al. (2013), Aerosol Optical Depth Value-Added Product, DOE/SC-ARM/TR-129,
229 USDOE Office of Science, Washington, D. C.
230

231 Kuo, Y. H., Schiro, K. A., & Neelin, J. D. (2018). Convective transition statistics over tropical
232 oceans for climate model diagnostics: Observational baseline. *J. Atmos. Sci.*, 75, 1553-1570.
233

234 Kuo, Y. H., Neelin, J. D., Chen, C. C., Chen, W.T, Donner, L. J., Gettelman, A, Jiang, X, Kuo,
235 K. T., Maloney, E., Mechoso, C. R., Ming, Y., Schiro, K. A., Seman, C. J., Wu, C. M., & Zhao,
236 M. (2020). Convective transition statistics over tropical oceans for climate model 2 diagnostics:
237 GCM evaluation, *J. Atmos. Sci.*, 77, 379-403.
238

239 Long, C. N. and Y. Shi, (2006): The QCRad Value Added Product: Surface Radiation
240 Measurement Quality Control Testing, Including Climatologically Configurable Limits,
241 Atmospheric Radiation Measurement Program Technical Report, ARM TR-074, 69 pp.
242

243 Long, C. N., and Y. Shi, (2008): An Automated Quality Assessment and Control Algorithm for
244 Surface Radiation Measurements, *TOASJ*, 2, 23-37, doi: 10.2174/1874282300802010023.
245

246 Maloney, E. D., Gettelman, A., Ming, Y., Neelin, J. D., Barrie, D., Mariotti, A., ... & Annamalai,
247 H. (2019). Process-Oriented Evaluation of Climate and Weather Forecasting Models. *Bulletin of*
248 *the American Meteorological Society*, 100(9), 1665-1686.
249
250 Pendergrass, A. G., & Hartmann, D. L. (2014). Two modes of change of the distribution of rain.
251 *Journal of Climate*, 27(22), 8357-8371.
252
253 Schiro, K. A., Neelin, J. D., Adams, D. K., & Lintner, B. R. (2016). Deep convection and column
254 water vapor over tropical land versus tropical ocean: A comparison between the Amazon and the
255 tropical western Pacific. *Journal of the Atmospheric Sciences*, 73(10), 4043-4063.
256
257 Taylor, K. E. (2001), Summarizing multiple aspects of model performance in a single diagram,
258 *J. Geophys. Res.*, 106(D7), 7183– 7192, doi:10.1029/2000JD900719.
259
260
261 Xie, S., Wang, Y. C., Lin, W., Ma, H. Y., Tang, Q., Tang, S., ... & Zhang, M. (2019). Improved
262 Diurnal Cycle of Precipitation in E3SM with a Revised Convective Triggering Function. *Journal*
263 *of Advances in Modeling Earth Systems*.
264
265 Xie, S., McCoy, R. B., Klein, S. A., Cederwall, R. T., Wiscombe, W. J., Jensen, M. P., ... &
266 Mather, J. H. (2010). Clouds and more: ARM climate modeling best estimate data: A new data
267 product for climate studies. *Bulletin of the American Meteorological Society*, 91(1), 13-20.
268
269 Xie, S. C., R. T. Cederwall, and M. H. Zhang (2004), Developing long-term single-column
270 model/cloud system-resolving model forcing data using numerical weather prediction products
271 constrained by surface and top of the atmosphere observations, *Journal of Geophysical Research-*
272 *Atmospheres*, 109(D1), doi: 10.1029/2003jd004045.
273
274 Zhang, C., and Xie, S., (2017). ARM Data-Oriented Metrics and Diagnostics Package for Climate
275 Model Evaluation Value-Added Product. Ed. by Robert Stafford, ARM Climate Research Facility.
276 DOE/SC-ARM-TR-202.
277
278 Zhang, C., Xie, S., Klein, S. A., Ma, H. Y., Tang, S., Van Weverberg, K., ... & Petch, J. (2018).
279 CAUSES: diagnosis of the summertime warm bias in CMIP5 climate models at the ARM southern
280 great plains site. *Journal of Geophysical Research: Atmospheres*, 123(6), 2968-2992.
281
282 Zhang, Y., Xie, S., Klein, S. A., Marchand, R., Kollias, P., Clothiaux, E. E., ... & Tang, S. (2018).
283 The ARM Cloud Radar Simulator for Global Climate Models: Bridging Field Data and Climate
284 Models. *Bulletin of the American Meteorological Society*, 99(1), 21-26.
285
286 Zhao, C., Xie, S., Klein, S. A., Protat, A., Shupe, M. D., McFarlane, S. A., ... & Hogan, R. J.
287 (2012). Toward understanding of differences in current cloud retrievals of ARM ground- based
288 measurements. *Journal of Geophysical Research: Atmospheres*, 117(D10).
289
290
291

292 Figure Captions Lists:

293

294 Figure 1: Annual cycle of monthly mean of (a) surface air temperature, (b) precipitation, (c) surface
295 air relative humidity, (d) surface downward shortwave radiative flux, (e) surface sensible flux, and
296 (f) surface latent heat flux over the ARM SGP domain (averaged over 35-38°N, 99-96°W) from
297 ARM observation averaged over 1999 to 2011 (red line with error bars representing one standard
298 deviation of inter-annual variability) and CMIP5 simulations averaged over 1979 to 2008 (grey
299 lines for individual CMIP5 models and black line for multi-model mean). JJA mean values are
300 shown in the legend. Plots are modified from Zhang et al. (2018).

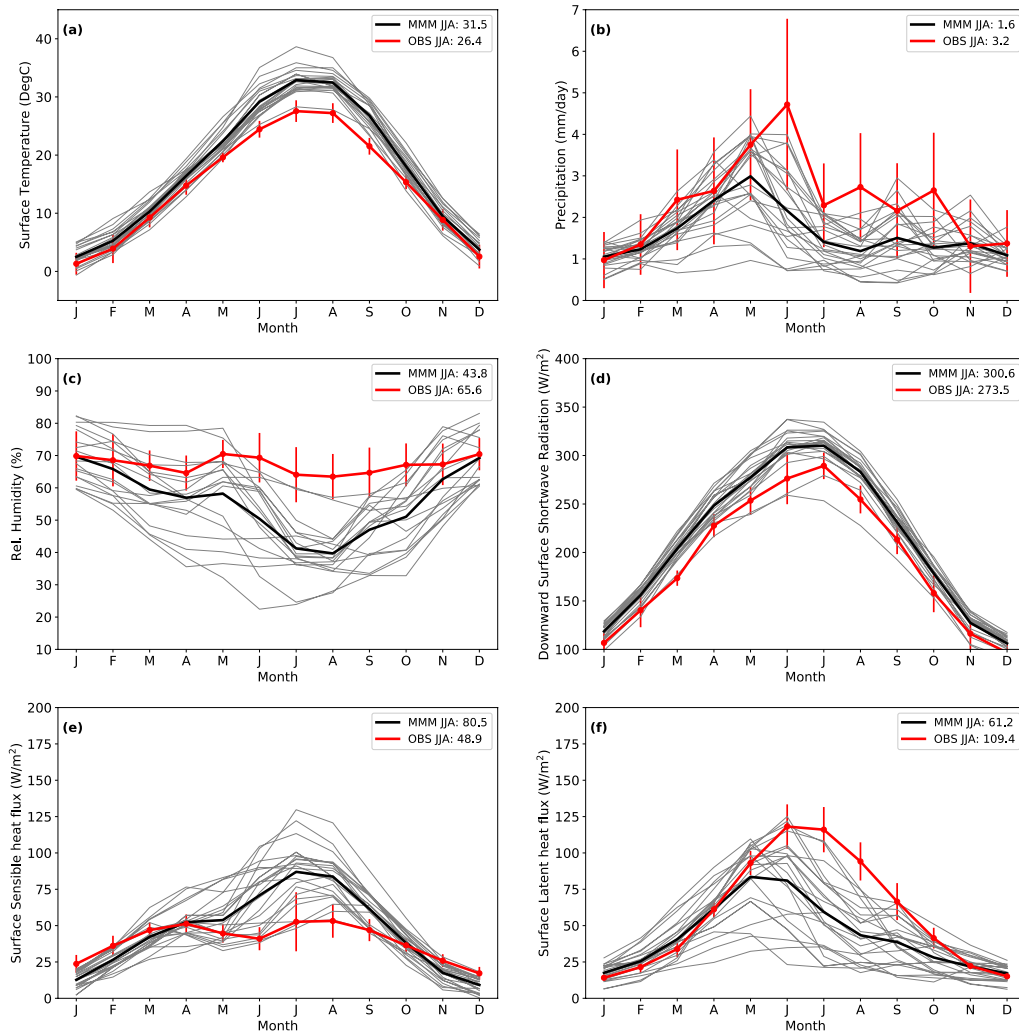
301 Figure 2: Climatological composite diurnal cycle of clouds from observed (left panel) and
302 simulated by E3SM (right panel). JJA mean at SGP (row 1); Annual mean at Manus (row 2).

303 Figure 3: Left: black dots are ARM observation. Curves are the first harmonics: grey for CMIP5
304 model AMIP type of runs. Color curves are from DOE's E3SM Atmosphere Model (EAM v1)
305 with a standard control run and a run using newly developed convection triggers (Detailed
306 experiment description can be found in (Xie et. al., 2019). Right: mapping precipitation peak
307 time and amplitude from the first harmonics to polar coordinate.

308

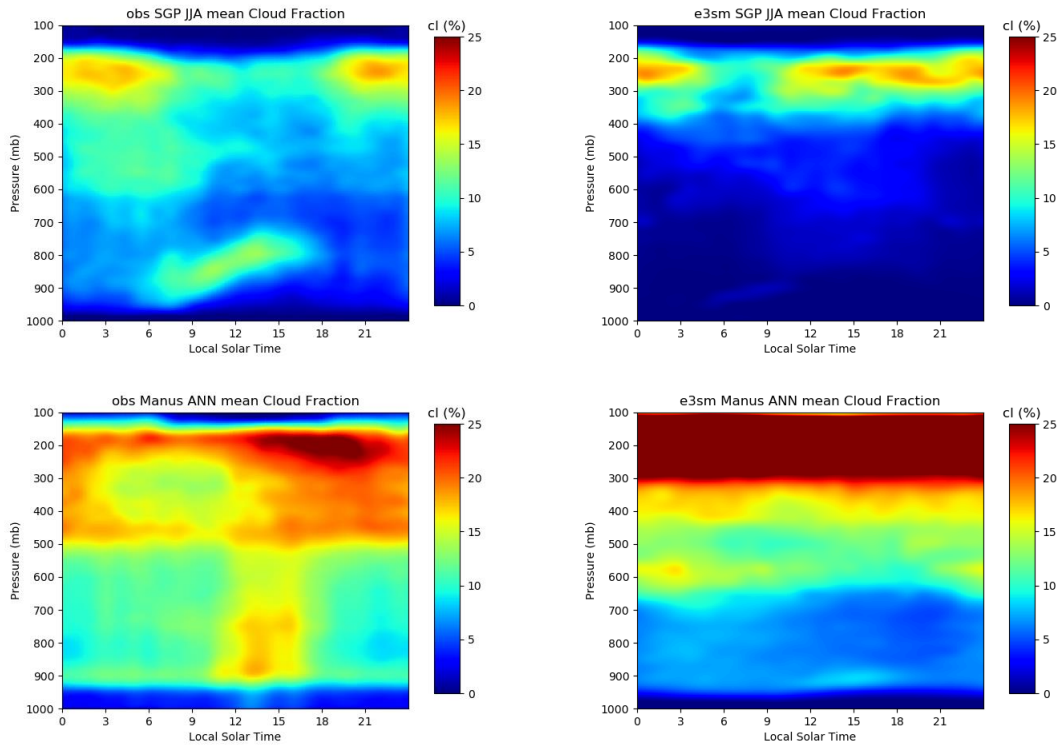
309 Figure 4: Daily-Mean precipitation frequency (a) and precipitation amount (b) as a function of
310 precipitation rate using observations from ARM (blue line) and GPCP (red line) compared with
311 CMIP5 AMIP simulations shown as gray lines. The black line represents the multi-model mean.
312 The precipitation bin arrangement follows method described by Pendergrass et al. (2014).

313 Figure 5: (a) Precipitation conditionally averaged on column water vapor (CWV) for observations
314 indicated by color-coded dots (ARMBE precipitation and gap filled MWRRET radiometer CWV)
315 and E3SM model output (black) over Manus Island. (b) as in (a) but for precipitation probability.
316 (c) The PDFs of CWV for observations (dark blue) and model (black) and of the contribution to
317 this from points with precipitation exceeding 0.5 mm/hr for observations (light blue) and model
318 (grey).
319



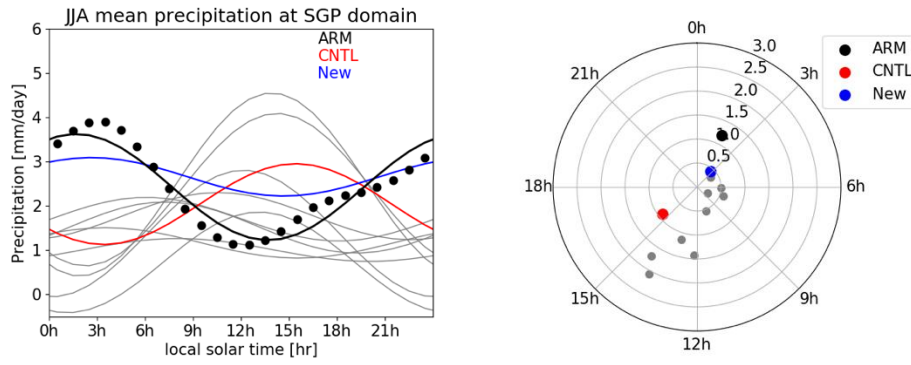
320
 321 Figure 1: Annual cycle of monthly mean of (a) surface air temperature, (b) precipitation, (c) surface
 322 air relative humidity, (d) surface downward shortwave radiative flux, (e) surface sensible flux, and
 323 (f) surface latent heat flux over the ARM SGP domain (averaged over 35-38°N, 99-96°W) from
 324 ARM observation averaged over 1999 to 2011 (red line with error bars representing one standard
 325 deviation of inter-annual variability) and CMIP5 simulations averaged over 1979 to 2008 (grey
 326 lines for individual CMIP5 models and black line for multi-model mean). JJA mean values are
 327 shown in the legend. Plots are modified from Zhang et al. (2018).

328



329 Figure 2: Climatological composite diurnal cycle of clouds from observed (left panel) and
 330 simulated by E3SM (right panel). JJA mean at SGP (row 1); Annual mean at Manus (row 2).

331



332

333 Figure 3: Left: black dots are ARM observation. Curves are the first harmonics: grey for CMIP5

334 model AMIP type of runs. Color curves are from DOE's E3SM Atmosphere Model (EAM v1)

335 with a standard control run and a run using newly developed convection triggers (Detailed

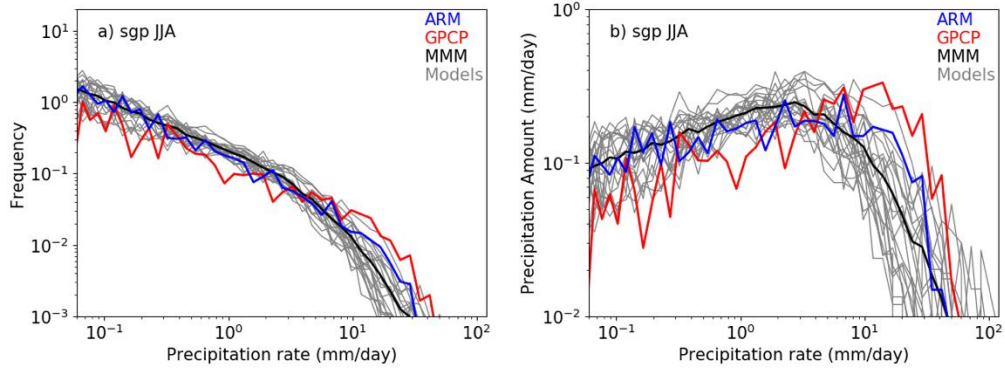
336 experiment description can be found in (Xie et. al., 2019). Right: mapping precipitation peak

337 time and amplitude from the first harmonics to polar coordinate.

338

339

340



341

342 Figure 4: Daily-Mean precipitation frequency (a) and precipitation amount (b) as a function of

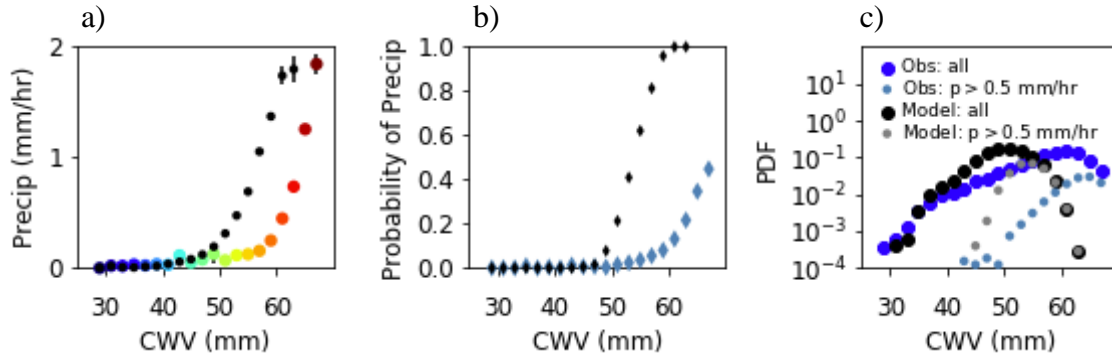
343 precipitation rate using observations from ARM (blue line) and GPCP (red line) compared with

344 CMIP5 AMIP simulations shown as gray lines. The black line represents the multi-model mean.

345 The precipitation bin arrangement follows method described by Pendergrass et al. (2014).

346

347



348 Figure 5: (a) Precipitation conditionally averaged on column water vapor (CWV) for observations
349 indicated by color-coded dots (ARMBE precipitation and gap filled MWRRET radiometer CWV)
350 and E3SM model output (black) over Manus Island. (b) as in (a) but for precipitation probability.
351 (c) The PDFs of CWV for observations (dark blue) and model (black) and of the contribution to
352 this from points with precipitation exceeding 0.5 mm/hr for observations (light blue) and model
353 (grey).

354

355 Table 1a

Quantities	M Data Products	Data Source/ Instruments	Time resolution	Spatial info
Surface Screen-Level Temperature/ Humidity	ARM Continuous forcing dataset	Surface Meteorological Observation System (SMOS), Oklahoma and Kansas mesonet stations (OKM and KAM)[Xie et al. 2004]	mon, day, hr	sgp domain averaged
Temperature/Humidity profile/wind speed/large scale tendencies	Same as above	NOAA/ NCEP Rapid Update Cycle (RUC) analysis data [Xie et al. 2004]	mon, day, hr	sgp domain averaged
Surface Precipitation	Same as above	Arkansas-Red Basin River Forecast Center (ABRFC) Nexrad radar precipitation estimates w/ rain gauge	mon, day, hr	sgp domain averaged
Precipitable Water	Same as above	Microwave Radiometer (MWR) water liquid & vapor along line of sight (LOS) path (MWRLOS)	mon, day, hr	sgp domain averaged
Surface All Sky Radiative Fluxes	Same as above	Data Quality Assessment for ARM Radiation Data (QCRAD) [Long and Shi, 2006, 2008]	mon, day, hr	sgp domain averaged
Aerosol Optical Depth 550nm	MFRSRAOD1M ICH	Multifilter Rotating Shadowband Radiometer (MFRSR) [Knoutz et al.,2013]	mon	Averaged over sgp Site C1 and E13
Surface Latent/Sensible Heat	BAEBBR	Best-Estimate Fluxes From EBBR Measurements and Bulk Aerodynamics Calculations (BAEBBR) [Cook, 2011a]	mon	sgp domain averaged
	QCECOR	Quality Controlled Eddy Correlation Flux Measurement [Cook, 2011b]	mon	sgp domain averaged
Surface Soil Moisture Content (10 cm)	SWATS	Soil Water and Temperature System (SWATS)) [Bond, 2005]	mon	sgp domain averaged
Cloud Fraction	ARSCL	Active Remote Sensing of Clouds [Clothiaux et al, 2001]	mon, day, hr	sgp Site C1
Ice Water Content/Liquid Water Content	ACRED	ARM Cloud Retrieval Ensemble Dataset [Zhao et al. 2012]	mon, day, hr	sgp Site C1

356

357

358

359 Table 1b

Quantities	ARM Data Products	Data Source/ Instruments	Time resolution	Spatial info
Surface Screen-Level Temperature/ Humidity	ARMBE-ATM	ARM-standard meteorological instrumentation at the surface [Xie et al. 2010]	mon	twp C1; nsa C1
Surface Precipitation	ARMBE-ATM	Same as above	mon, hr	twp C1; nsa C1
Precipitable Water	ARMBE-ATM	Microwave Radiometers Retrievals (MWRRET) [Xie et al. 2010]	mon, hr	twp C1; nsa C1
Surface Radiative Fluxes	ARMBE-CLD	Data Quality Assessment for ARM Radiation Data (QCRAD) [Long and Shi, 2006, 2008]	mon	twp C1; nsa C1
Cloud Fraction	ARSCL	Active Remote Sensing of Clouds [Clothiaux et al, 2001]	mon, hr	twp C1; nsa C1

360

361 Table 1: Observed quantities selected in the evaluation package, including the quantity names,

362 the data sources, and the temporal and spatial information of the data. (a) for SGP and (b) for

363 NSA and TWP sites.